AIAA'86

AIAA-86-1892
PROPELLER NOISE CAUSED BY
BLADE TIP RADIAL FORCES

D.B. HANSON
HAMILTON STANDARD
WINDSOR LOCKS, CT.

AIAA 10th Aeroacoustics Conference
July 9-11, 1986/Seattle, Washington

PROPELLER NOISE CAUSED BY BLADE TIP RADIAL FORCES

Donald B. Hanson*

Acoustics and Noise Control
Hamilton Standard
Division of United Technologies Corporation
Windsor Locks, Connecticut 06096

Abstract

Accurate prediction of propeller noise requires knowledge of this aerodynamic loading distribution on the blades, particularly in the tip region. An aspect of tip flow that has been neglected in noise work is the radial suction force generated when air flows from the lower (pressure) surface of the blade around the tip to the upper surface. This radial force is an inescapable consequence of producing lift and, in theory, is not diminished by reducing tip thickness. The tip flow may separate and re-attach on the suction surface producing an extra force component known in wing aerodynamics as vortex lift. This paper examines new experimental evidence of vortex flow at the tip edges and at the leading edges of Prop-Fans and addresses the performance and noise consequences. It is concluded that the tip edge vortex is an important noise source, particularly for unswept Prop-Fan blades. In preliminary calculations for single rotation Prop-Fans at take off conditions, adding the tip side edge source improved the agreement between experiment and theory at blade passing frequency. At high speed conditions such as the Prop-Fan cruise point, it was found analytically that the tip loading effect tends to cancel thickness noise.

Nomenclature

b	= local blade chord
B	= number of blades
B_0	= chord/diameter
BPF	= blade passing frequency
C_L	= section lift coefficient
c_0	= ambient speed of sound
f	= shape of chordwise load distribution
FA,MCA	= face alignment, mid chord alignment - see other Hanson references
g_r	= source component from equations in Ref. 10
$J_{mB}(x)$	= Bessel function
J_{mB}	= $(d/dx)J_{mB}$
k_x	= chordwise wavenumber - Eq. 6
K	= loading constant - Eq. 15
LAP	= Large scale Advanced Prop-Fan
m	= harmonic order
M_r	= section relative Mach number
M_T	= section rotational Mach number
r, r_0, r_T	= observer, source, tip radius

s	= tip side edge force/unit length
t_b	= blade section thickness/chord ratio
U	= blade section relative speed
U_T	= U at tip
X	= chordwise dsitance/chord, $0 \leq X \leq 1$
y	= sideline distance to observer
z	= radius ratio r_0/r_T
δ	= Dirac delta function
ξ_0, γ_0	= distance normal, parallel to local advance direction
θ	= angle to observer measured from flight axis
ρ_0	= ambient density
$\Psi_V(k_x), \Psi_1(k_x),$ $\Psi_R(k_x)$	= chordwise Fourier transforms of thickness, lift, radial load distributions. In each case $\Psi(0) = 1$ (for compact source).

Introduction

Most modern propeller noise theory is based on the acoustic analogy whereby the noise field can be computed by evaluating certain integrals of source terms on and around the blades. The linear sources are given by the blade geometry, for thickness noise, and by the blade pressure distribution, for loading noise. Evaluation of the source integrals, assuming the source distributions are known, is reasonably straightforward and several methods are available.[1] However, for the swept, low aspect ratio, transonic blades typical of Prop-Fans, estimation of the loading source distribution is difficult and undoubtedly limits accuracy of noise predictions.

Aerodynamic methods to determine blade loading for Prop-Fans are mostly based on the assumption of fully attached flow. Noise predictions using this type of aerodynamics have been reasonably good for single rotation propellers at high tip speed where thickness noise is dominant. But at low speed, high power coefficient conditions typical of Prop-Fan take-off, predictions tend to be low, as indicated by Figure 1*. Agreement for

---

*Because of rig power limitations, much of the testing reported in Reference 2 was with 2 blades rather than the design value of 8 blades. The reference shows that the BPF harmonic (8P or 8 per rev) for an 8-blade configuration is given accurately by the 8P harmonic of the 2-blade test + $20\log_{\infty}(8/2) = 12$dB. Thus, Figure 1 and some later figures show the 8P harmonic as representative of BPF.

---

*Principal Research Engineer, Aircraft Systems Division Associate Fellow AIAA

1

these conditions could not be improved substantially by making any reasonable change to the lift and drag dipole distributions and Mach numbers were too low for significant quadrupole contribution. The magnitude of this underprediction suggests that a significant source component may be missing from the theory. An explanation for this discrepancy has been discovered in recent analytical and experimental work at Hamilton Standard and United Technologies Research Center which shows that vortex flow of the type well known for swept wing aircraft (Figure 2) occurs on Prop-Fan blades at low forward speed conditions including take-off.
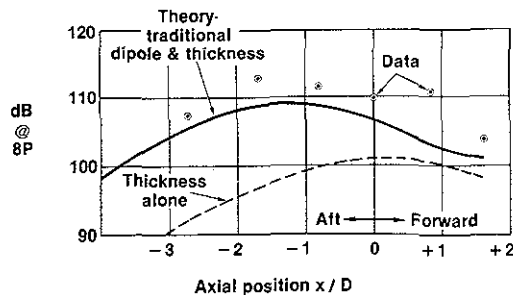

Fig. 1 Underprediction of noise using traditional source components for a Prop-Fan at low tip speed, high power condition typical of take-off. Data from 2 blade SR-3 model simulates BPF of 8 blade propeller at $M_X = 0.2$, $M_T = 0.89$, and power coefficient = 0.69. Sideline distance = 4.9 diameters. (Data: Ref. 2, Run 329)

This paper reveals some of the early indications of the vortex flow phenomenon on Prop-Fans and explores the noise and loading implications. The next section gives some physical description of vortex flow based on wing experience and then shows evidence for Prop-Fans. Succeeding sections present analytical methods for loading and noise, predicted noise trends, and a sample calculation compared with the data from Reference 2.

Background from Wing Aerodynamics

The vortex flow pattern shown in Figure 2 is for a delta wing at low speed. A vortex sheet separates at the leading edge and re-attaches in a manner to produce high lift under the vortex due to its low pressure. Downstream of the reattachment line the suction is reduced to a level predictable for potential flow. A simplified view of the leading edge condition for a flat plate airfoil is sketched in Figure 3. For potential flow, shown at the top, the upper streamline approaches stagnation under the airfoil and then moves forward and around the leading edge without separation. The high acceleration around the edge produces a suction force on the airfoil edge in the direction shown that is finite despite the vanishingly small frontal area. This leading edge thrust, or suction, is vital in reducing induced drag on 3-D wings. For wings with small leading edge radii and sufficient sweep, the flow cannot stay attached at the leading edge but separates

and re-attaches as suggested in the lower part of Figure 3 (and in Figure 2). On delta wing aircraft, vortex flow is used to produce high lift coefficients for landing without flaps; but in cruise it is reduced or eliminated by operating at lower incidence.
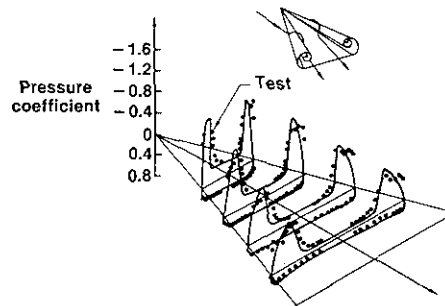

Fig. 2 Vortex flow pattern and pressure distribution for delta wing aircraft. Aspect ratio 1.46, angle of attack 14°. (Ref. 3, with permission)
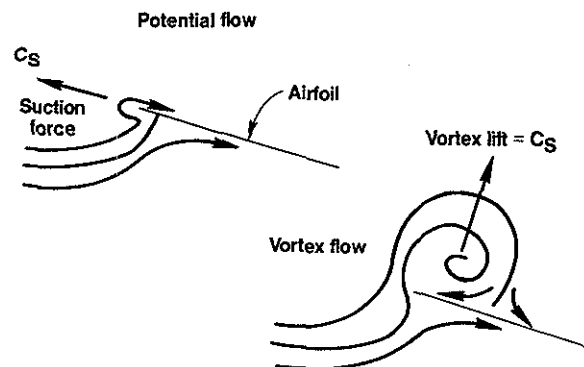

Fig. 3 Idealized view of leading edge flow conditions for 2-D flat plate airfoil. (Ref. 3, with permission)

On wings with squared off tips, a similar pattern can occur at the side edges as suggested in Figure 4. The lift distribution dropping to zero at the tip causes a spanwise flow component outward underneath and inward above. Under ideal conditions, the flow stays attached as it wraps around the tip; however, if the lift is too high or if the tip is too thin, the flow will separate and form a vortex on the upper surface as shown below in Figure 4. Without separation the flow produces a spanwise suction force which has no impact on performance because it has no component in either the lift or drag direction. If the vortex forms on the upper surface, it produces extra lift beyond that which would be computed for potential flow. Figure 5 shows, via Werlé's flow visualization,[4] a mixture of these two conditions: attached flow toward the leading edge and a vortex rolled up on the upper surface after the mid chord.
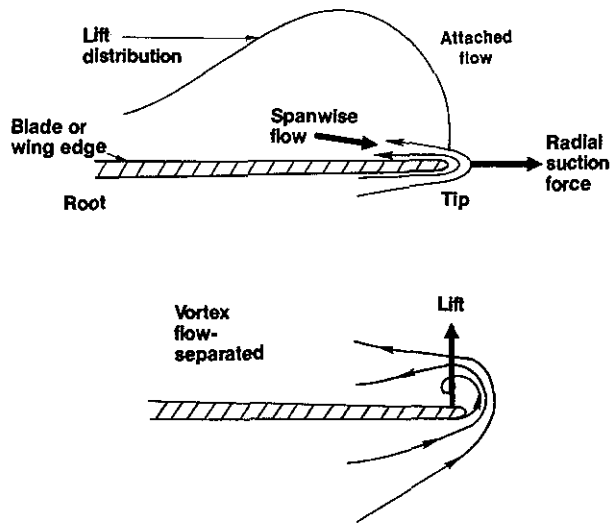
2

Fig. 4 Tip edge vortex flow

Fig. 5 Flow visualization at tip of wing with NACA
0012 airfoil at 12° angle of attack. Test
in water with dye injection. (Photo by
Werlé, Ref. 4, with permission)

Figure 6 gives an idea of how much extra lift can be caused by leading edge and side edge vortices. The curve labeled "potential flow" was computed with a panel method under the assumption of attached flow. The additional lift associated with the leading edge vortex was computed via the "suction analogy".[6],[7] In this method the leading edge suction or thrust is computed using a panel method; then at high angle of attack the thrust rotates to the lift direction as in Figure 4. The side edge lift is calculated by a similar procedure. Figure 6 shows that lift can be doubled by vortex effects on low aspect ratio, swept wings.
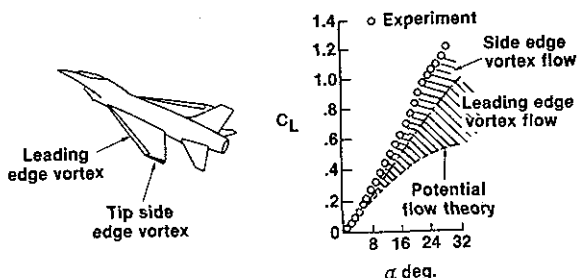

Fig. 6 Extra lift caused by vortex flow (Ref. 5,
with permission

Evidence of Vortex Flow on Prop-Fans

Attached tip vortices on the upper surfaces of straight helicopter rotors[8] and propeller blades[9] have been known for some time via experimental work in the 1970s although their implications for harmonic noise do not seem to have been explored before. More recent blade pressure and flow visualization tests reveal the presence of both tip and leading edge vortices for Prop-Fans as described below.

Blade surface pressures were measured under NASA funding in April 1986 on the 9 ft. diameter LAP propeller shown in Figure 7. For these measurements a Scanivalve™ was connected to 15 tubes under the surface of each face of a specially manufactured blade. Pressure distributions in Figure 8 for a takeoff simulation clearly show evidence of the vortex at the tip station on the upper surface. At 18° and $r/R = 0.99$ (upper left panel in Figure 8) the appearance of the vortex loading hump at mid-chord is consistent with the roll-up onto the upper surface shown for a wing in Figure 5. With increasing incidence, the vortex seems to move toward the leading edge and eventually disappears, possibly lifting off the tip.

The presence of leading edge vortices on air propellers was not suspected until recently because most analytical methods have tended to over-predict power absorption. Extra lift due to attached vortices would have widened the gap between test and theory. Then in 1985 the propeller aerodynamic method PROP-PAN (for propeller panel) described in references 10 and 11 was upgraded under NASA funding from vortex lattice to true lifting surface. Power calculations based on attached flow matched data well at the design point although the slope of the power curve versus blade angle was low relative to measurements. Chordwise pressure distributions for two extreme loading conditions are shown in Figures 9 and 10 along with tuft patterns photographed in the United Technologies Research Center main wind tunnel in 1983. The high positive leading edge loading condition exhibits a tuft pattern suggestive of vortex flow on the suction surface; the high negative loading seems to produce vortex flow on the pressure surface as would be expected from wing experience.
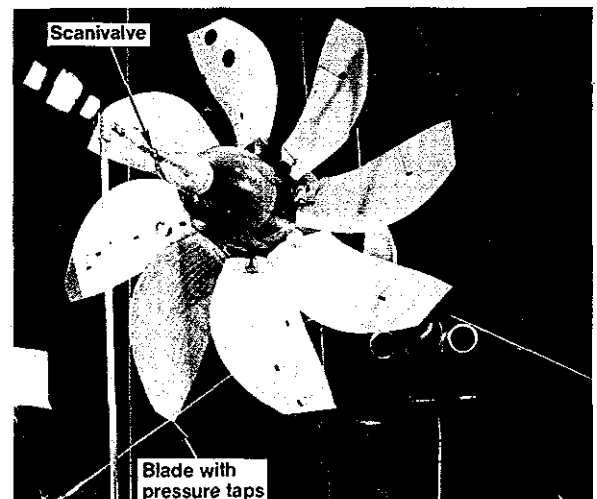

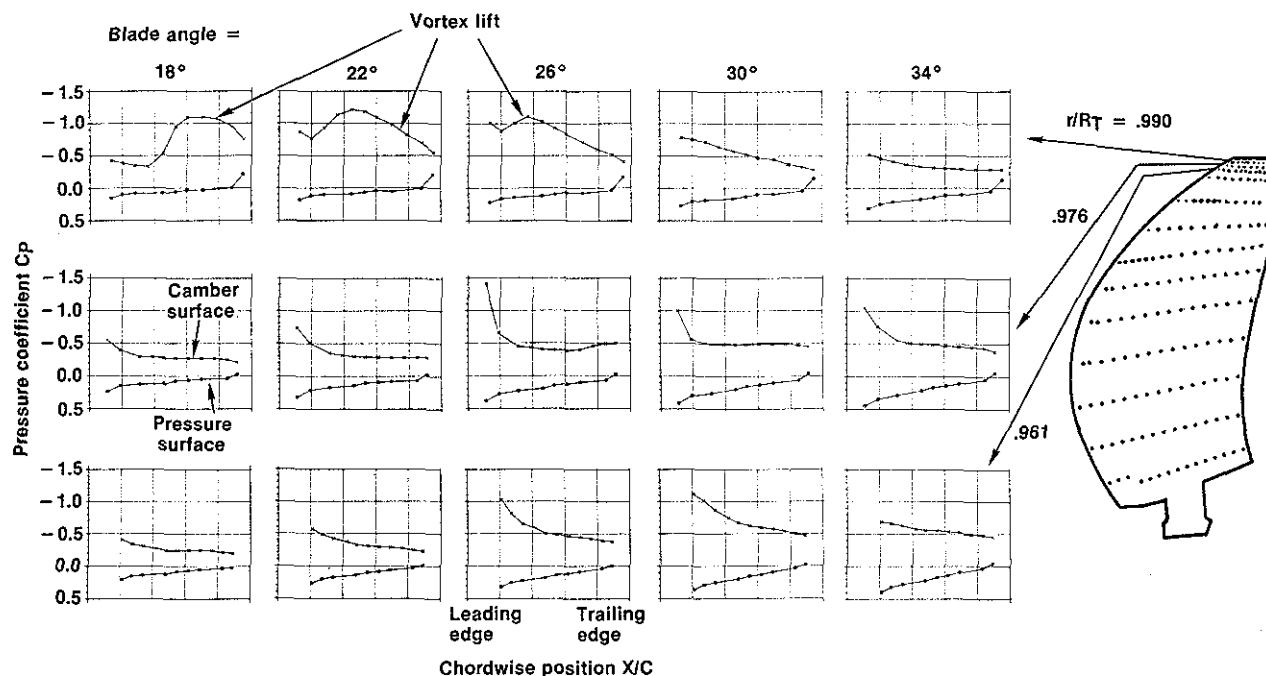Fig. 7 LAP propeller with taps on one blade for
steady pressure measurement

3

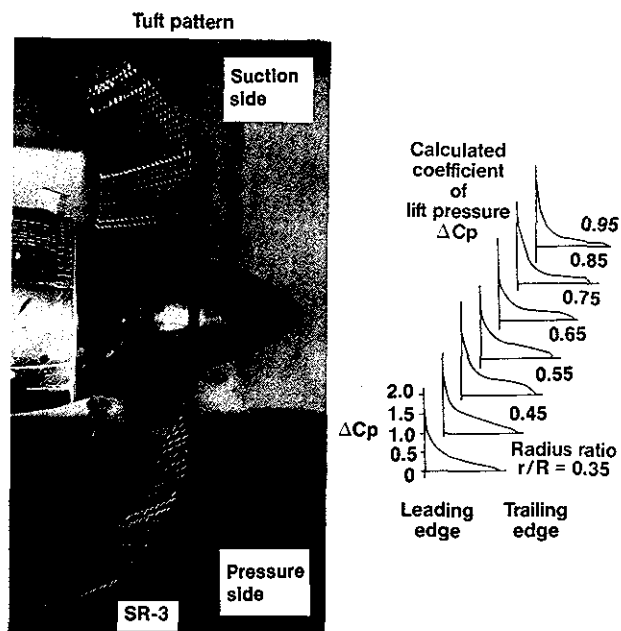Fig. 8 Blade pressure measurements in tip region at 0.5 advance ratio

Tuft pattern

Fig. 9 SR-3 take-off condition (J = 0.88, M = 0.2,
Blade angle 42°). Lift pressure calculated
with lifting surface theory shows high
positive leading edge loading. Tufts
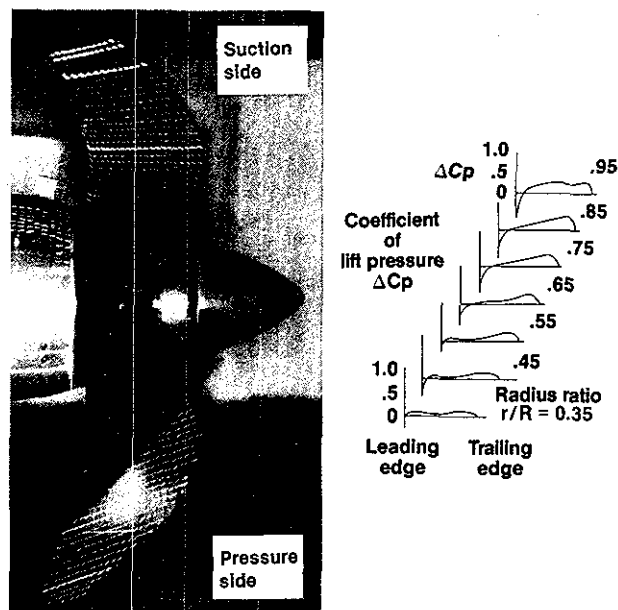suggest leading edge vortex on suction
side (upper blade)

Fig. 10 SR-3 at high advance ratio condition (J = 4.3,
M = 8.0, blade angle 60°). Calculated
lift pressure shows negative leading edge
loading. Tufts suggest leading edge vortex
on pressure side (lower blade).

4

Dr. Lawrence Bober of NASA-Lewis pointed out that leading edge vortices have been investigated on marine propellers and directed the author to the paper[12] containing Figure 11. This picture actually represents a blade untwisted for a non-rotating test in a water tunnel. The results shown in the preceding figures led Hamilton Standard to enlist the help of flow visualization experts at UTRC to search for leading edge vortices on the counter-rotation propeller under test in the UTRC Acoustic Research Tunnel. A pattern shown by their oil film/fluorescent tracer method is shown in Figure 12. Although the streaks are mostly radial, a distinct change in streak direction is shown along the line corresponding to vortex reattachment in Figure 11. This pattern on the suction surface of the front rotor was for the CPRX1 take-off condition, which is predicted by the counter-rotation PROP-PAN program to have high leading edge loading similar to that shown in Figure 9. For the windmilling condition (zero shaft power) where negative leading edge loading is expected, the vortex pattern appeared on the opposite surface.
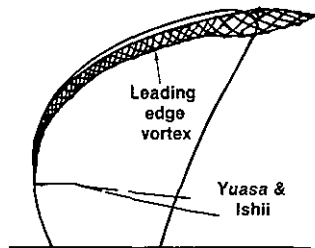

Fig. 11 Vortex flow visualization on a simulated marine propeller in a water tunnel.
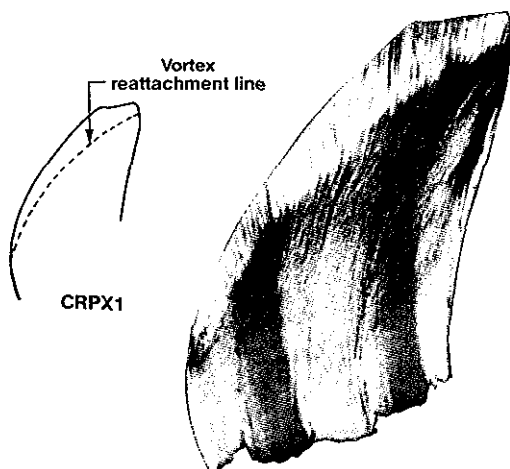(Ref. 10, with permission of publisher)

Fig. 12 Flow visualization results for CRPX1 at take off condition. Change in streak direction indicates vortex reattachment line

Thus, it is clear that leading edge and side edge vortices play an important role in Prop-Fan aerodynamics. In retrospect, this should have been expected because Prop-Fans have the design features known to be critical in wing experience: low aspect ratio, sharp edges, and sweep. Conventional propellers, which typically have thicker, unswept, higher aspect ratio blades, should be less affected by vortex flow.

Noise Theory for Radial Loading

For noise calculations, lift and drag sources are usually included in a way to assure that the integrated propeller thrust and torque are essentially correct. Thus, the leading edge suction force is included at least in a crude sense. With regard to radial loading, Farassat and Martin[13] evaluated the effect of tip side edge suction on noise of lightly loaded helicopter rotors and concluded that it was small but not negligible. The suction studied in their paper is caused by thickness which, of course, diminishes with thickness ratio. Source strength was evaluated with a 2-D transonic airfoil code.

By contrast, the suction referred to in this paper is the inevitable result of producing lift on a 3-D wing or blade and must be evaluated with 3-D aerodynamics. Thinning the blade has the effect of increasing the local negative pressure in a way such that the pressure times the effective edge area (i.e., the integrated force) tends to be preserved in the limit as the thickness approaches zero.[14] The major effect of thinning is to reorient the suction force from the edgewise direction to the lift direction as in Figure 4. The radial tip loading associated with lift seems to have been ignored in the past and thus should be examined as a "new" source. This section presents far-field frequency domain radiation theory for radial tip loading and examines behavior of the noise component compared to thickness noise.

The foundation for the radial loading noise theory was laid in reference 10 in which a general radiation integral was given for any helically convected source, steady or unsteady. The generalized source included the volume displacement (monopole); lift, drag, and radial dipole components; and the quadrupole term. All of the sources but the radial dipole have been explored in previous papers by the author.

For radial tip loading, the appropriate source component can be written

$$g_r = \partial/\partial r_0 [s(\gamma_0)\delta(r_T - r_0)\delta(\xi_0 + FA)] \qquad (1)$$

where $s(\gamma_0)$ is the force per unit length distributed along the tip chord line. Chordwise distance is measured approximately here along the helical advance coordinate γ_0. Delta functions $\delta(r_T - r_0)\delta(\xi + FA)$ locate the line of action of the source at the intersection of the cylinder of radius r_T and the helicoidal surface defined by the advance of the propeller tip.

A radial force coefficient C_R can be defined according to

$$s(\gamma_0) = (\rho_0 U_T^2/2)r_r \; S[(\gamma_0 - MCA)/b]C_R \qquad (2)$$

where MCA is the sweep. The function S gives the shape of the chordwise distribution and is normalized to unit area according to

$$\int_{CHORD} S(\gamma_0/b) \; d(\gamma_0/b) = 1 \qquad (3)$$

Thus, the integrated radial force is $(\rho_0 U_T^2/2)br_rC_R$ where U_T is the tip helical speed. With these definitions, the radial loading noise harmonic P_{Rm} can be found by carrying the derivation through as in Reference 11 while including the g_r source term to find a near-field expression. The far field formula below is obtained by the method of stationary phase as was used for thickness noise in the appendix of Reference 15.

$$P_{Rm} = \frac{-\rho_0 c_0^2 B \sin\theta \, \exp\left[imB\left(\dfrac{\Omega_0 r}{c_0} - \dfrac{\pi}{2}\right)\right]}{8\pi\left(\dfrac{y}{D}\right)(1-M_x\cos\theta)} \; M_r^2 \exp[i(\phi_0+\phi_s)]$$

$$\cdot \; J_{mB}'\left(\frac{mBM_r\sin\theta}{1-M_x\cos\theta}\right) M_r k_x \sin\theta \left(\frac{C_R}{2}\right) \Psi_R(k_x) \qquad (4)$$

where Ψ_R is the frequency domain source representation defined by

$$\Psi_R(k_x) = \int_{-\infty}^{\infty} S(X)\exp(ik_x X)dX \qquad (5)$$

k_x is the chordwise wavenumber from previous papers[16],[17]:

$$k_x = \frac{2mBB_D M_T}{M_r(1-M_x\cos\theta)} \qquad (6)$$

From equations 3, 5, and 6 it can be seen that Ψ_R approaches unity for low harmonic order m or small tip chord B_D. ϕ_0 and ϕ_s are the phase lags associated with offset and sweep as in the references and are given by

$$\phi_0 = \frac{2mB}{zM_r}\left(\frac{M_r^2\cos\theta - M_x}{1 - M_x\cos\theta}\right)\frac{FA}{D} \qquad (7)$$

$$\phi_s = \frac{2mBM_T}{M_r(1 - M_x\cos\theta)}\left(\frac{MCA}{D}\right) \qquad (8)$$

(For the tip sources, M_r assumes the tip value and $z = 1$.)

Equation 4 is the major analytical result of this paper. It was written in a form for direct comparison with the volume displacement and lift noise harmonics derived in reference 17 as

$$\begin{Bmatrix} P_{Vm} \\ \\ P_{Lm} \end{Bmatrix} = \frac{-\rho_0 c_0^2 B \sin\theta \exp\left[imB\left(\dfrac{\Omega_0 r}{c_0} - \dfrac{\pi}{2}\right)\right]}{8\pi\left(\dfrac{y}{D}\right)(1 - M_x\cos\theta)} \qquad (9)$$

$$\times \int_{root}^{tip} M_r^2\exp[i(\phi_0+\phi_s)] \; J_{mB}\left(\frac{mBzM_r\sin\theta}{1 - M_x\cos\theta}\right) \begin{Bmatrix} k_x^2 t_b \Psi_V(k_x) \\ \\ ik_y(C_L/2)\Psi_L(k_x) \end{Bmatrix} dz$$

The k_y wavenumber is defined by

$$k_y = \left(\frac{2mBB_D}{zM_r} \; \frac{M_x - M_r^2\cos\theta}{1 - M_x\cos\theta}\right) \qquad (10)$$

with a sign convention reversed from some of the author's earlier references.

Lowson was probably the first to study radial force as a blade noise source. The aerodynamic origin of his source was in the coning of helicopter main rotors in which the force is distributed along the blade span, not concentrated at the tip. (Coning is the tendency of the hinged blades to sweep out a cone rather than a disc due to the vertical load.) Acoustically, however, the sources are equivalent and Equation 4 can be reduced to Lowson's point source hover case (his Equation A-10) by setting M_x, ϕ_0, and ϕ_s to 0 and Ψ_R to 1 (for compactness).

Before proceeding to aerodynamic loading calculations, it is worth studying some general properties of the above noise equations. It can be seen from forms of Equations 4 and 9 that the radial load source radiates with a directivity very much like that of volume displacement. But the radiation efficiency of the former is governed by J_{mB}' and the latter by J_{mB}. Simply plotting representative Bessel functions leads to some intriguing conclusions. Figure 13 shows the appropriate J and J' for an 8-blade Prop-Fan at BPF and design advance ratio. Ranges of the abcissa are indicated for flight Mach numbers of 0.6 and 0.8 and visual angles between 70° and 110°. For Mach numbers less than 0.8, the two noise components are additive. For higher Mach numbers they tend to cancel, actually reducing overall noise. This is a possible explanation for the observation that linear theories (without the radial loading source) tend to underpredict at low Mach number and overpredict at high Mach number.

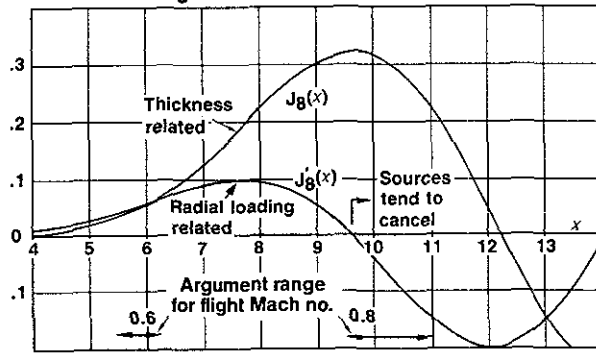J = 3.06   mB = 8 $\theta = 90° \pm 20°$
Flight Mach No. = 0.6 and 0.8

Fig. 13 Bessel function properties for thickness
and radial loading sources. Augment
$x = mB\ M_T \sin\theta/(1 - M_X \cos\theta)$ where θ
is the radiation angle. Augment ranges
for visual angles $70° \rightarrow 110°$ and advance
ratio = 3.06.

This conjecture can be given a little more substance by calculating the ratio

$$\Delta dB = 20\ \log_{10}\left(\frac{P_{Vm} + P_{Rm}}{P_{Vm}}\right) \qquad (11)$$

which represents the noise added to the thickness source by the radial loading. This is plotted in Figure 14 based on the following assumptions, which seem reasonable based on experience. A radial loading coefficient $C_R = 0.02$ was used for all Mach numbers. The thickness noise integral was computed via an effective radius approximation with $r_{eff} = 0.8r_T$, *thickness/chord* = .02 and *chord/diameter* = .11. The figure shows that the sources are additive at all directivities for Mach numbers up to 0.7 with more of an effect behind the plane of rotation. At $M_X = 0.8$ there is little effect except in the aft quadrant. Because of the approximations involved, these results must *be considered indicative only; a more precise example is given later in the paper.* Note also that the radial loading noise component was compared with the thickness component because the two have similar forms; however, thickness will not be the dominant noise source at lower Mach numbers.

- SR-2 design J and blade angle
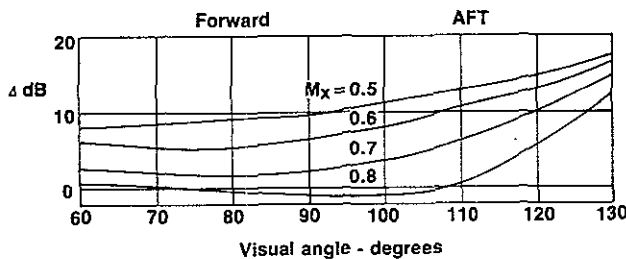- Varying flight mach no. $-M_X$

Fig. 14 Increment to thickness noise due to radial
loading source. Thickness component
based on effective radius representation
with advance ratio = 3.06

Aerodynamic Loading Methods

To apply the acoustic equations just derived, the radial tip loading can be estimated by adapting aerodynamic methods originally developed for wings. A whole spectrum of methods is available to deal with vortex flow and many papers on the subject are available. Interested readers are directed particularly to an AGARD Conference Proceedings on vortex flow,[19] a review paper by Parker,[20] and two papers by Kulfan.[3,21] Available methods include parabolized NavierStokes, Euler, full potential, linear surface potential, and lifting surface panel methods. For acoustics and overall performance considerations, a simple method that works well for integrated loading is appropriate even if detailed flow information is not provided. The obvious choice here is the "suction analogy" method, developed originally by Polhamus,[6] Lamar,[7] and others in which leading edge and tip edge suction forces are computed based on loading from linear panel methods. The analogy states that the magnitude of these forces is the same regardless of whether they act in the edgewise direction or normal to the lifting surface.

In this paper, calculations are presented for the tip edge force only; leading edge forces are left to a future report. The analytical method closely parallels that given in Lamar's original work[7] in which the suction force per unit length is given by

$$s(\gamma_0) = \pi\rho_0 G^2(\gamma_0) \qquad (12)$$

where G is the limit, approaching the tip, of the product of the radial velocity and the square root of the distance from the tip.

$$G(\gamma_0) = \sqrt{r_T}\ \lim_{z\rightarrow 1}\sqrt{1-z}\ v_r \qquad (13)$$

The radial velocity is related to the bound vorticity $(U/2)\Delta Cp$ by

$$v_r = (1/2r_T)(\partial/\partial_z)\int_{\gamma_{LE}}^{\gamma_0} (U/2)\Delta C_p(\gamma_0')d\gamma_0' \qquad (14)$$

A good fit to the computed pressure distribution near the tip is given by the expression

$$\Delta Cp(\gamma_0') = Kf(X_0)\sqrt{1-z^2} \qquad (15)$$

where $X_0 = \gamma_0'/b$. The chordwise distribution f is arbitrary at this point. $1-z^2$ gives the required elliptic loading behavior near the tip. K is a constant to be found by fitting Equation 15 to a potential flow calculation.

Combining equations 14 and 15 and performing the indicated operations yields the expression for v_r

$$v_r = \frac{Ukb}{4r_T}\ \frac{-z}{\sqrt{1-z^2}}\ g(X) \qquad (16)$$

where

$$g(X) = \int_0^X f(X_0)dX_0 \qquad (17)$$

7

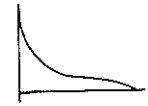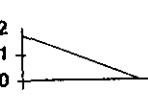Equations 12, 13 and 16 can be combined to give the edge force distribution
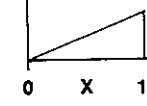
$$s(\gamma_0) = \frac{\pi \rho_0}{32 r_T} U^2 b^2 K^2 g^2(X) \qquad (18)$$

Finally, the radial force coefficient is obtained by integrating this expression over the tip chord and normalizing by $(1/2)\rho_0 U^2 b r_T$

$$C_R = (\pi/4)K^2 B_0^2 \int_0^1 g^2(X) dX \qquad (19)$$

Some properties of this expression are worth noting before presenting numerical results. First, C_R is proportional to the square of tip loading (given by K). Hence, high tip loading is to be avoided. Second, the chordwise load distribution f has a strong effect on $\int g^2(X)dX$. To illustrate this point, Table I gives values of the integral for 5 idealized f functions.

Table I Effect on radial loading of chordwise pressure distribution shape

f(X)	$\int_0^1 g^2(X)\,dX$
$\delta(X)$	1.000
$(2/\pi)\sqrt{(1-X)/X}$	.615
$2(1-X)$	.533
1	.333
2X	.200

It can be seen that the radial force is highest when the chordwise distribution is concentrated at the leading edge and diminishes continuously as the loading concentration is moved aft. The high leading edge loading shown in Figure 9 is typical for calculated take-off conditions and is reasonably well approximated by the flat plate loading shape $\sqrt{(1-X)/X}$ given in the table.

Sample Calculation

In Reference 2 it was found that theory with thickness and traditional lift and drag dipoles under-predicted the data at the lowest Mach numbers tested. The example shown in Figure 1 is for swept blades; for unswept blades, the underprediction is greater as shown for SR-2 at the same power and RPM in Figure 15. The thickness noise component is shown in Figure 1 to be only a minor contributor and transonic non-linear effects are expected to be small at these test conditions. In this section, aerodynamic and noise calculations are presented indicating that the tip suction force is the major cause of the underprediction. SR-2 is treated first because the leading edge vortex is probably less of an issue.
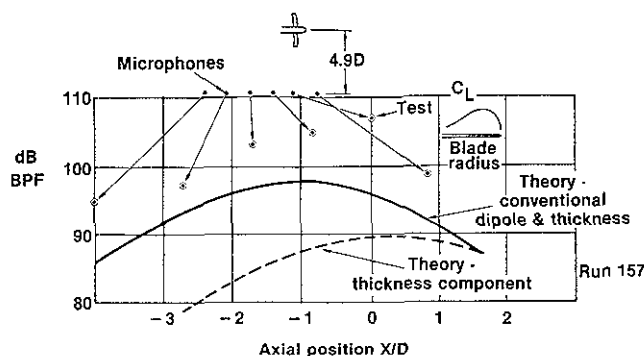

Fig. 15 Underprediction of noise using traditional sources for SR-2 (unswept) Prop-Fan. Data from Ref. 2, Run 157

For the aerodynamic calculations, the PROP-PAN program predicted the lift loading on SR-2 shown in Figure 16. The integrated power was found to be 29% lower than the measured value. Under the assumption that this was due to a blade angle error, the loading was adjusted upward by 29% uniformly over the blades*. The SR-2 blade planform is rounded at the tip starting at $z \sim 0.93$. Because it was felt that the simple radial loading model outlined above could not cope adequately with rounded tips, the planform was considered rectangular for calculation of vortex loading. The tip chord value was taken to be that the $z = 0.95$ ($B_0 = 0.12$). To evaluate K in the expression for C_R, Equation 15 was integrated to yield

$$K = C_L(z)/\sqrt{1 - z^2} \qquad (20)$$

---

*A better explanation for this may be that the extra loading arises from a leading edge vortex caused by rotation. This possibility is being explored.
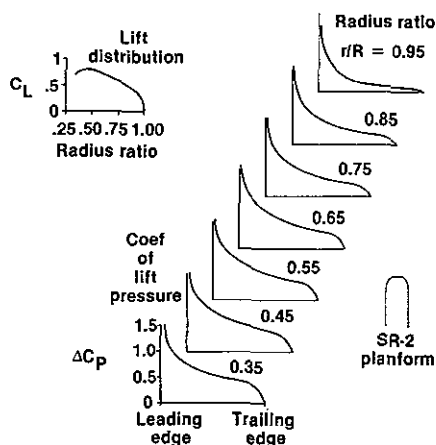
Fig. 16 Predicted blade loading for SR-2 Prop-Fan
based on lifting surface theory without
vortex separation

By using the predicted C_L at either of the outer 2 control point radii ($z = 0.85$ or 0.95), K for this point was found to be 1.5. If the chordwise loading factor is assumed to lie midway between the first 2 curves in Table I, the value of C_R is estimated as .025.

This value of C_R was used with Equation 4 to predict the noise at 8 times the rotation frequency, simulating blade passing frequency for an 8-blade Prop-Fan. Figure 17 repeats the original under-prediction curve from Figure 15 and also shows the level with the radial dipole added. The peak level is increased 4 dB, considerably improving the prediction.
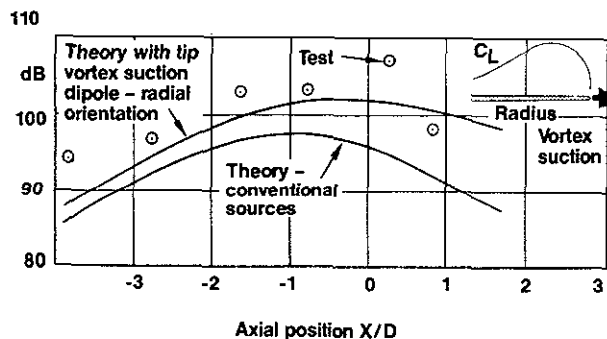

Fig. 17 Improved predictions for SR-2 using vortex
suction in radial direction

A check was made to find the effect of orienting the tip vortex load in the lift direction rather than the radial direction as shown in Figure 5. The result shown in Figure 18 indicates that, for the same force magnitude, the lift source is a much less efficient than the radial load source. Thus, based on comparison with the noise data, the dominant loading seems to be radial although there is probably some roll-up onto the upper surface.
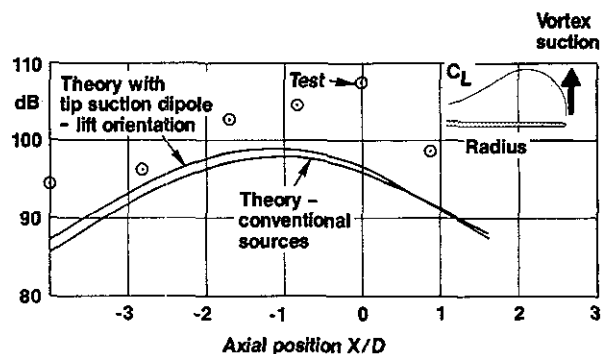

Fig. 18 Prediction for SR-2 assuming vortex suction
acts on blade tip in lift direction

Finally, similar calculations were made for the SR-3 model for the condition represented in Figure 1. The results shown in Figure 19 lead to different conclusions than those for the unswept blade. If the tip suction force is assumed to act in the radial direction, the noise is overpredicted; if it is assumed in the lift direction, the prediction is low. In comparison with the straight blade results, it seems likely that the tip suction loading is more on the blade upper surface. This is plausible considering the flow pattern indicated in Figure 12, which was for a similar blade at similar conditions.
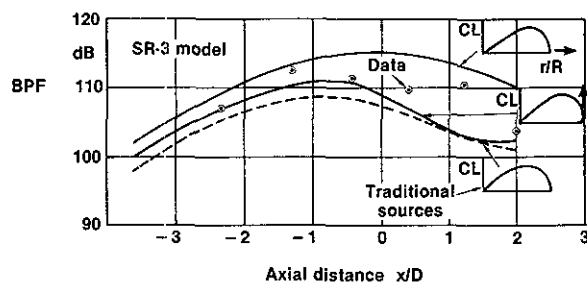

Fig. 19 Tip suction contributions to noise of SR-3
(swept) model. Dashed curve and data
reproduced from Figure 1

Blade sweep has been recognized for some time as a noise reduction feature for high Mach number cruise conditions because of its relief of transonic effects and its de-phasing of harmonic noise radiation. In light of the present work, it now appears that sweep may help at take-off conditions as well by rotating the tip suction loading away from the radial direction more toward the lift direction.

Conclusion

Experimental evidence from two flow visualization methods and from blade pressure taps clearly indicates the presence of leading edge and tip edge vortex flow on Prop-Fans. Loading conditions under which these appear correspond to those well known from wing aerodynamics. In the tip area,

9

the acceleration associated with the air flowing outward on the pressure side of the blade, wrapping around the tip, and then flowing inward on the suction surface produces a radial suction force whose dipole radiation has an important influence on noise. At low speeds, typical of take-off, this new source radiates in phase with thickness noise and is likely to be an important noise source, particularly for unswept blades. For swept blades the influence is diminished, apparently because of a re-orientation of the tip suction force away from the radial direction. At higher speeds, the radial source is out of phase with thickness noise and may actually provide an overall noise reduction. Much more work is needed for better understanding of vortex loading effects on propeller noise. Particularly challenging areas will be the influence of sweep and the treatment of unsteady flow.

Acknowledgements

Figure Credits

Figures 2, 3 and 5 are copyrighted by the American Institute of Aeronautics and Astronautics; reprinted with permission.

Figure 5 was first published in AGARD Conference Proceedings 342, Paper 8 by the Advisory Group for Aerospace Research and Development, North Atlantic Treaty Organization (AGARD/NATO) 1983.

Figure 11 is reproduced with permission of Hemisphere Publishing Corp, New York, N.Y.

References

1. Farassat, F., "Linear Acoustic Formulas for Calculation of Rotating Blade Noise," AIAA Journal, Vol. 19, Sept. 1981, p. 1122.

2. Brooks, B.M. and Metzger, F.B., "Acoustic Test Analysis of Three Advanced Turboprop Models", NASA CR-149667, 1980.

3. Kulfan, R.M., "Wing Airfoil Shape Effects on the Development of Leading Edge Vortices", AIAA Paper No. 79-1675.

4. Werlé, H., "Visualization des Ecoulements Tourbillonnaires Tridimensionnels", Aerodynamics of Vortical Type Flows in Three Dimensions, AGARD CP-342, 1983.

5. Lamar, J.E., "Prediction of Vortex Flow Characteristics of Subsonic and Supersonic Speeds", J. Aircraft, Vol. 13, No. 7, p. 490, 1976.

6. Polhamus, E.C., "A Concept of the Vortex Lift of Sharp-Edge Delta Wings Based on a Leading-Edge-Suction Analogy", NASA TN D-3767, 1966.

7. Lamar, J.E., "Extension of Leading-Edge-Suction Analogy to Wings with Separated Flow Around the Side Edges at Subsonic Speeds", NASA TR R-428, 1974.

8. Gray, R.B., McMahon, H.M., Shenoy, K.R., and Hammer, M.L., "Surface Pressure Measurements at Two Tips of a Model Helicopter Rotor in Hover", NASA CR-3281, 1980.

9. Gilmore, D.C., "Surface Pressure Measurements on a Propeller Blade Operating at Zero Advance Ratio", Air Force Flight Dynamics Report AFFDL-TR-71-88, Vol. V, September, 1971.

10. Hanson, D.B., "Compressible Helicoidal Surface Theory for Propeller Aerodynamics and Noise", AIAA Journal, Vol. 21, No. 6, June 1983, p. 881.

11. Hanson, D.B., "Compressible Lifting Surface Theory for Propeller Performance Calculation", Journal of Aircraft, Vol. 22, No. 1, January 1985, p. 19.

12. Yuasa, H. and Ishii, N., "Leading Edge Separating Vortex and Pressure Distributions on Propeller Blades", Proceedings of the Second International Symposium on Flow Visualization, Bochum, West Germany, Sept. 1980, p. 256, Hemisphere Publishing Corp, New York, 1982.

13. Farassat, F. and Martin, "A Note on the Tip Noise of Rotating Blades", J. Sound and Vibration, Vol. 86, 1983, pp. 449-453.

14. Jones, R.T. and Cohen, D., High Speed Wing Theory, Princeton University Press, Princeton, N.J., 1960.

15. Hanson, D.B., "Near-Field Frequency-Domain Theory for Propeller Noise", AIAA Journal, Vol. 23, April 1985, pp. 499 - 504.

16. Hanson, D.B., "Helicoidal Surface Theory for Harmonic Noise of Propellers in the Far Field", AIAA Journal, Vol. 18, No. 10, October 1980, p. 1213.

17. Hanson, D.B., "Influence of Propeller Design Parameters on Far-Field Harmonic Noise in Forward Flight", AIAA Journal, Vol, 18, No. 11, November 1980, p. 1313.

18. Lowson, M.V., "Basic Mechanisms of Noise Generation by Helicopters, V/STOL Aircraft and Ground Effect Machines", J. Sound and Vibration, Vol. 3, No. 3, 1966, p. 454.

19. Aerodynamics of Vortical Type Flows in Three Dimensions, AGARD Conference Proceedings CP 342, 1983.

20. Parker, A.G., "Aerodynamic Characteristics of Slender Wings with Sharp Leading Edges - A Review", J. Aircraft, Vol. 13, No. 3, 1976, p. 161.

21. Kulfan, R.M., "Wing Geometry Effects on Leading Edge Vortices," AIAA Paper 79-1872, 1979.

10